Research Square

Preprints are preliminary reports that have not undergone peer review.
They should not be considered conclusive, used to inform clinical practice,
or referenced by the media as validated information.

Dual Targeting of MiRNA-21 and PI3K/AKT by Honokiol Overcomes Paclitaxel Resistance in Triple-Negative Breast Cancer

Seyed Mohammad Jafar Haeri
Arak University of Medical Sciences
Zeynab Saleh
Arak University of Medical Sciences
Hadi Karami
hadimolmed@gmail.com

Arak University of Medical Sciences

Research Article

Keywords: Drug Synergism, Honokiol, MicroRNAs, Paclitaxel, Triple-Negative Breast Neoplasms

Posted Date: September 22nd, 2026

DOI: https://doi.org/10.21203/rs.3.rs-10985637/v1

License: This work is licensed under a Creative Commons Attribution 4.0 International License.
Read Full License

Additional Declarations: No competing interests reported.

Abstract

Background

Triple-negative breast cancer (TNBC) is aggressive and frequently develops paclitaxel resistance. The oncomiR miRNA-21 promotes chemoresistance by targeting PTEN and PDCD4. Honokiol, a natural lignan, modulates miRNAs and enhances chemosensitivity. This study investigated whether honokiol sensitizes TNBC cells to paclitaxel via the miRNA-21/PTEN/PI3K/AKT axis.

Methods

MDA-MB-231 and MDA-MB-468 cells were treated with honokiol, paclitaxel, or their combination at IC_{50} doses. Cytotoxicity was assessed by MTT and combination index (CI) analysis. Proliferation, migration, colony formation, apoptosis, and gene/protein expression were evaluated using trypan blue, wound healing, colony formation, Hoechst/ELISA/caspase-3, qRT-PCR, and Western blotting.

Results

Honokiol and paclitaxel synergistically reduced cell viability (CI < 1), with IC_{50} values decreasing from 6.22 to 4.21 μM (MDA-MB-231) and 5.03 to 3.21 μM (MDA-MB-468). Combination suppressed migration (to 44.5% and 32.5%) and colony formation (29% and 31%). Honokiol downregulated miRNA-21, and upregulated PTEN/PDCD4, were reversing paclitaxel-induced miRNA-21 elevation. Combination reduced phospho-AKT, cyclin D1, and MMP-2. Apoptosis was enhanced (caspase-3: 2.46 and 2.62 fold).

Conclusions

Honokiol overcomes paclitaxel resistance in TNBC by modulating miRNA-21/PTEN/PI3K/AKT signaling, offering a promising combination strategy.

Introduction

Breast cancer remains the most frequently diagnosed malignancy and the leading cause of cancer-related mortality among women worldwide, with an estimated 2.3 million new cases and 670,000 deaths reported globally in 2022 [1, 2]. Despite significant advances in early detection and therapeutic strategies, the management of breast cancer, particularly triple-negative breast cancer (TNBC), continues to present substantial clinical challenges due to its aggressive nature, high metastatic potential, and propensity for developing chemoresistance [3]. Paclitaxel, a microtubule-stabilizing agent, remains a cornerstone chemotherapeutic drug in the treatment of breast cancer, demonstrating remarkable antitumor efficacy through the inhibition of mitotic spindle dynamics [4]. However, the

clinical utility of paclitaxel is severely hampered by the frequent development of acquired or intrinsic drug resistance, which represents a major obstacle to successful treatment outcomes and contributes to disease recurrence [5]. The mechanisms underlying paclitaxel resistance are multifactorial and include enhanced drug efflux, alterations in microtubule dynamics, dysregulation of apoptotic pathways, and activation of survival signaling cascades [6]. These complex resistance mechanisms underscore the urgent need for developing novel therapeutic strategies that can circumvent chemoresistance and improve patient outcomes.

MicroRNAs have emerged as critical regulators of cancer progression and drug resistance in breast cancer [7]. Among the numerous miRNAs implicated in breast cancer pathogenesis, miR-21 has garnered particular attention as one of the most consistently overexpressed oncomiRs in human malignancies [8]. MiRNA-21 is frequently upregulated in breast cancer tissues compared to normal counterparts and is associated with aggressive tumor behavior, poor prognosis, and resistance to chemotherapy [9]. Mechanistically, miRNA-21 promotes tumorigenesis and chemoresistance by targeting multiple tumor suppressor genes, including phosphatase and tensin homolog (PTEN) and programmed cell death 4 (PDCD4) [10, 11]. PTEN, a negative regulator of the PI3K/AKT signaling pathway, is a well-established direct target of miRNA-21, and its downregulation leads to constitutive activation of the PI3K/AKT/mTOR cascade, promoting cell survival, proliferation, and drug resistance [12]. PDCD4, another critical miRNA-21 target, functions as a tumor suppressor by inhibiting translation and promoting apoptosis; its suppression by miRNA-21 contributes to malignant transformation and therapy resistance. Importantly, studies have demonstrated that miRNA-21 inhibition significantly enhances the chemotherapeutic effect of paclitaxel in breast carcinoma cells, highlighting miRNA-21 as a promising therapeutic target for overcoming paclitaxel resistance [13].

Honokiol, a naturally occurring bioactive biphenolic compound isolated from the stem and root bark of *Magnolia officinalis*, has emerged as a promising anticancer agent with pleiotropic effects on multiple cellular signaling pathways [14]. Extensive preclinical studies have demonstrated that honokiol exerts potent antitumor activities against various cancer types, including breast cancer, through the induction of apoptosis, inhibition of proliferation, suppression of migration and invasion, and enhancement of chemosensitivity [15]. Mechanistically, honokiol has been shown to induce apoptosis through modulation of Bcl-2 family proteins, increasing the expression of pro-apoptotic proteins while decreasing anti-apoptotic proteins, leading to caspase activation and PARP cleavage [16]. Honokiol also inhibits EGFR signaling and potently suppresses NF-κB activation, further contributing to its anticancer effects [17]. Notably, recent evidence has demonstrated that honokiol can modulate miRNA expression, particularly through the downregulation of miRNA-21. In human osteosarcoma cells, honokiol was shown to suppress proliferation and induce apoptosis via regulation of the miRNA-21/PTEN/PI3K/AKT signaling pathway [18]. A recent study demonstrated that honokiol exhibits significant antitumor effects in breast cancer by modulating the miRNA-148a-5p-CYP1B1 axis and showed a strong synergistic effect between honokiol and paclitaxel in vitro [19]. Honokiol has also been reported to antagonize doxorubicin resistance in human breast cancer via the miRNA-188-5p/FBXW7/c-Myc pathway, further supporting its role in modulating miRNA-mediated chemoresistance [20].

Despite the well-established anticancer activities of honokiol and its emerging role in miRNA modulation, the potential effects of honokiol on miRNA-21 expression, its downstream target genes (PTEN and PDCD4), and the consequent impact on paclitaxel sensitivity in breast cancer cells remain poorly understood. Given the critical role of miRNA-21 in breast cancer progression and paclitaxel resistance, honokiol-mediated downregulation of miRNA-21 may represent a novel therapeutic strategy to overcome chemoresistance and enhance the efficacy of paclitaxel-based chemotherapy. Therefore, the present study aims to comprehensively investigate the effects of honokiol on miRNA-21 expression, its downstream target genes (cyclin-D1, MMP-2, PTEN and PDCD4), and paclitaxel sensitivity in breast cancer cells under in vitro conditions. Furthermore, we seek to evaluate whether honokiol can enhance the chemosensitivity of breast cancer cells to paclitaxel through modulation of the miRNA-21/PTEN/PI3K/AKT signaling axis, potentially providing a rationale for developing novel combination therapeutic strategies for breast cancer management.

Materials and methods

Cell culture

The MDA-MB-231 and MDA-MB-468 breast cancer cell lines, both procured from the Pasteur Institute in Tehran, Iran, were seeded in RPMI-1640 growth medium (Gibco, USA). The medium was supplemented with 10% fetal bovine serum (FBS, Gibco), 2 mM L-glutamine, 100 U/mL penicillin, and 100 µg/mL streptomycin (Gibco). The cells were subsequently maintained at 37°C in a humidified incubator gassed with 5% CO_2.

MTT assay

The MTT assay was used to test paclitaxel and honokiol, individually and combined, against MDA-MB-231 and MDA-MB-468 cells across five groups: blank, solvent, paclitaxel (0–32 µM), honokiol (0–32 µM), and paclitaxel + honokiol (0–32 µM). Cells were plated in 96-well plates at 5 × 10^3/well, treated for 24 h, and then incubated with 10 µL of MTT (5 mg/mL; Sigma-Aldrich, St. Louis, MO, USA) for 4 h at 37°C. Formazan crystals were dissolved in 150 µL DMSO per well. Absorbance was read at 490 nm using an ELISA plate reader (Awareness Technology, Palm City, FL, USA). Survival percentages were calculated relative to controls, and IC_{50} values were determined using GraphPad Prism software (GraphPad Software Inc., San Diego, CA, USA). In all subsequent experiments, we used the compounds at their IC_{50} concentrations.

Combination index (CI) analysis

We investigated the combined effect of honokiol and paclitaxel through a CI analysis following the Chou-Talalay protocol [21, 22]. After transforming the MTT results into fractional affected (Fa) scores, with Fa = 0 indicating full cell survival and Fa = 1 indicating total cytotoxicity, we processed the data using

CompuSyn software (Combosyn, Paramus, NJ, USA). The resulting CI values served as the basis for determining synergy (CI < 1), additivity (CI = 1), or antagonism (CI > 1).

Cell proliferation assay

Trypan blue dye exclusion was utilized to investigate the anti-proliferative effects of honokiol and paclitaxel, alone and in combination, on breast cancer cells. The cells were seeded at 4×10^4 cells/well in 6-well plates and treated with their respective IC_{50} doses for 24 to 120 hours. Post-incubation, the cells were trypsinized and stained with an equal volume of 0.4% trypan blue (Merck KGaA, Darmstadt, Germany) for 3 minutes. A hemocytometer and inverted microscope (Nikon Instrument Inc., Melville, NY, USA) were used for cell counting, with viability expressed as the proportion of unstained viable cells to the total counted

Quantitative real-time PCR (qRT-PCR)

We performed qRT-PCR to evaluate how treatments modulate gene expression at the RNA level. After 24 h of treatment, total cellular RNA was harvested with a commercially available RNA isolation kit (Parstous, Tehran, Iran) and subsequently converted to cDNA using the Easy cDNA Synthesis Kit (Parstous). For the amplification step, reactions were run on a Roche LightCycler 96 instrument using SYBR Green MasterMix (Parstous). The reaction mixture was prepared with a total volume of 20 µL, containing 10 µL of SYBR Green MasterMix, 6 µL of nuclease-free water, 1 µL of forward and reverse primers each, and 2 µL of the cDNA template. The primer pairs utilized are presented in Table 1. The cycling protocol included an initial activation at 95°C for 10 minutes, followed by 35 amplification cycles: denaturation at 95°C for 15 seconds, primer annealing at 58°C for 40 seconds, and polymerization at 72°C for 35 seconds. Data analysis was performed using the standard $2^{-\Delta\Delta Ct}$ threshold cycle method [23, 24], normalizing target gene expression to the housekeeping gene.

Table 1
Primer sequences used for qRT-PCR

Genes	Sequence (5'→3')	Primer length (base)	Tm (º C)
β-actin FW	GACATCCGCAAAGACCTGTA	20	57.62
β-actin RV	GGAGCAATGATCTTGATCTTCA	22	56.22
MiRNA-21 FW	GGGGGGTAGCTTATCAGACTG	21	58.31
MiRNA-21 RV	CAGTGCGTGTCGTGGAGT	18	58.94
PTEN FW	AGAAAGCTTACAGTTGGGCCCTGT	24	64.37
PTEN RV	GCCACAGCAAAGAATGGTGATGCT	24	64.44
PDCD4 FW	GGGAGTGACGCCCTTAGAAG	20	59.82
PDCD4 RV	ACCTTTCTTTGGTAGTCCCCTT	22	58.94
Cyclin D1 FW	CAATGACCCCGCACGATTTC	20	59.87
Cyclin D1 RV	CATGGAGGGCGGATTGGAA	19	58.87
MMP-2 FW	CAGGCTCTTCTCCTTTCACAAC	22	59.19
MMP-2 RV	AAGCCACGGCTTGGTTTTCCTC	22	63.86
FW: Forward, RV: Reverse			

Western blotting

Protein extracts were prepared from cellular lysates, and their concentrations were assessed via the BCA protein assay (Pierce Biotechnology, Inc., Rockford, IL, USA). Samples containing 30–50 μg of protein per lane were loaded onto 10–15% SDS-PAGE gels, electrophoretically separated, and subsequently transferred onto nitrocellulose membranes (GE Healthcare Bio-Sciences, Pittsburgh, PA, USA). To prevent background staining, the membranes were blocked with 5% (w/v) nonfat milk powder for 1 hour, and then incubated at 4°C overnight with a panel of primary antibodies: mouse monoclonal anti-AKT (1:1000), rabbit monoclonal anti-phospho-AKT (1:1000), and rabbit monoclonal anti-β-actin (1:1000). Following primary antibody incubation, the membranes were exposed for 1 hour to secondary IgG antibodies, goat anti-rabbit (1:3000) or horse anti-mouse (1:4000). Final detection of the protein bands was achieved using the SuperSignal™ West Pico Chemiluminescent Substrate (Thermo Fisher Scientific, Waltham, MA, USA).

Migration assay

To assess migratory capacity, we performed a wound-healing assay on confluent breast cancer cell monolayers in 6-well plates. After generating a consistent scratch with a sterile 200-µL pipette tip and washing away detached cells with PBS, we treated the cultures with 500 µL of fresh RPMI-1640 containing IC_{50} doses of honokiol and paclitaxel, alone or in combination, for 24 h. At 24 h after treatment onset, we photographed three random fields per well. Migratory activity was determined by measuring wound-width reduction and normalizing each experimental group against the untreated control.

Colony formation assay

To assess the long-term proliferative potential of breast cancer cells after drug exposure, we performed a clonogenic (colony formation) assay. Cells were plated at a density of 1×10^4 cells per well in 6-well plates and exposed to IC_{50} concentrations of honokiol and paclitaxel for 24 hours. The treatment medium was then replaced with fresh culture medium, and the plates were incubated for two weeks to permit colony development. Upon completion of the incubation, colonies were fixed and stained with 0.4% crystal violet. Quantification was carried out by counting the stained colonies using ImageJ software (National Institutes of Health, USA), and the colony counts for each treatment group were compared with those of the untreated control.

Hoechst staining

The capacity of honokiol and paclitaxel, used either as stand-alone therapies or in combination, to induce apoptosis in breast cancer cells was examined through Hoechst 33342 staining. Cells were first plated in 12--well dishes at a density of 1×10^5 per well and allowed to attach for 24 hours. Subsequently, they were exposed to IC_{50} concentrations of the drugs for a further 24 hours. Post-treatment, the cells were washed twice with PBS, fixed using 3.7% formaldehyde, and incubated with Hoechst 33342 (5 µg/mL) for 30 minutes. Apoptotic nuclei were then identified via fluorescence microscopy based on distinctive morphological criteria, including chromatin condensation, pyknosis, and nuclear disintegration.

ELISA cell death assay

The induction of apoptosis was assessed using a commercial ELISA kit (Roche Diagnostics GmbH) that detects cytoplasmic mono- and oligonucleosomes, specific hallmarks of apoptotic cell death. Breast cancer cells were plated in 24-well dishes at a density of 1×10^5 cells/well and incubated for 24 h with IC_{50} concentrations of honokiol, paclitaxel, or their combination. Following lysis and centrifugation, 20-µL aliquots of the cleared supernatants were mixed with 80 µL of a detection immunoreagent (anti-DNA-POD plus anti-histone-biotin) and transferred to streptavidin-coated plates. The plates were kept at 25°C for 2 h, rinsed, and then developed with 100 µL of ABTS substrate per well. The colorimetric reaction was halted with stop solution, and the optical density was measured at 405 nm using a microplate reader (Awareness Technology). The extent of apoptosis was determined by calculating the fold-increase in absorbance relative to the untreated control group.

Caspase-3 activity assay

Caspase-3 activity was determined in breast cancer cells using a colorimetric detection kit (Abnova, Taipei, Taiwan), with procedures performed as outlined by the manufacturer. The cells were first lysed in 50 µL of lysis buffer, followed by centrifugation at 10,000 rpm to discard any particulate matter. The resulting supernatants were then reacted with a prepared mixture consisting of 50 µL of 2X reaction buffer (containing 10 mM DTT) and 5 µL of the specific chromogenic substrate DEVD-pNA (4 mM). After a 2 h incubation period at 37°C, the absorbance was read at 405 nm. The measured optical density, indicative of p-nitroaniline release, served as a direct reflection of caspase-3 activity within the treated cell populations.

Statistical Analysis

Values are reported as mean ± standard deviation from no fewer than three independent experiments, each carried out in triplicate. The unpaired Student's t-test served for pairwise comparisons, while one- or two-way ANOVA followed by Tukey's or Dunnett's post-hoc test was employed for multi-group analyses, as appropriate. A threshold of $p < 0.05$ indicated statistical significance.

Results

Honokiol potentiates paclitaxel-induced cytotoxicity in breast cancer cells

To investigate the effect of honokiol on the sensitivity of breast cancer cells to paclitaxel, combination treatments were performed on both MDA-MB-231 and MDA-MB-468 cells using an MTT cytotoxicity assay. Treatment with either honokiol or paclitaxel alone clearly decreased cell survival in a dose-dependent manner across both cell lines ($p < 0.05$, relative to untreated controls). The IC_{50} values for honokiol in MDA-MB-231 and MDA-MB-468 cells were 17.56 µM and 13.33 µM, respectively, while paclitaxel alone exhibited IC_{50} values of 6.22 µM and 5.03 µM, respectively, indicating that MDA-MB-468 cells were slightly more sensitive to both single agents than MDA-MB-231 cells (Fig. 1a and 1b). Notably, the combination of honokiol with paclitaxel further decreased cell survival in both cell lines, reducing the IC_{50} values to 4.21 µM in MDA-MB-231 and 3.21 µM in MDA-MB-468 cells ($p < 0.05$, relative to single-agent therapies). These data indicate that honokiol can increase the sensitivity of breast cancer cells to paclitaxel in both triple-negative breast cancer models, with the combination yielding a more pronounced effect than either agent alone.

Synergistic antiproliferative effects of honokiol and paclitaxel in breast cancer cell lines

CI analysis revealed synergistic antiproliferative interactions (CI < 1) between honokiol and paclitaxel across both MDA-MB-231 and MDA-MB-468 cell lines, with CI values ranging from 0.69 to 0.92 (Fig. 1c

and 1d). In MDA-MB-231 cells, synergism was observed across all tested fractional affected (Fa) levels. The most pronounced effect occurred at Fa = 0.76 with a CI of 0.70, and a CI of 0.72 was noted at Fa = 0.83. At lower Fa values, CI values remained below 1.0 (0.92–0.87 at Fa = 0.11–0.25), indicating consistent synergy. In MDA-MB-468 cells, CI values also remained below 1.0 throughout. The strongest synergy was observed at Fa = 0.89 with a CI of 0.69, followed by Fa = 0.82 (CI = 0.74) and Fa = 0.63 (CI = 0.75). Even at the lowest Fa tested (0.16), the CI was 0.84, confirming synergism. Collectively, these results demonstrate that honokiol and paclitaxel act synergistically in both breast cancer cell lines, with the greatest efficacy observed at higher fractional inhibition levels.

Honokiol enhances paclitaxel-mediated growth inhibition in MDA-MB-231 and MDA-MB-468 cells

To assess the antiproliferative activities of honokiol and paclitaxel, alone or in combination, MDA-MB-231 and MDA-MB-468 cells were treated and monitored over a period of 120 hours. Cell viability was normalized to the untreated control at each respective time point. The solvent control had no observable effect on proliferation in either cell line, maintaining 100% viability throughout the experiment, confirming the absence of vehicle-induced cytotoxicity. In MDA-MB-231 cells, honokiol induced a gradual, time-dependent reduction in viability, decreasing from 78.65% at 24 hours to 40.62% at 120 hours. Paclitaxel monotherapy demonstrated stronger inhibitory activity, with viability falling to 71.23% at 24 hours and reaching 27.58% by 120 hours. Notably, the honokiol + paclitaxel combination yielded the most pronounced effect, reducing viability to 58.84% at 24 hours, 49.90% at 48 hours, 41.27% at 72 hours, 32.16% at 96 hours, and 25.49% at 120 hours, respectively (Fig. 1e and 1f). Comparable trends were observed in MDA-MB-468 cells. Honokiol alone reduced viability from 75.43% (24 hours) to 40.75% (120 hours), while paclitaxel alone resulted in a decline from 67.48% to 31.57% over the same period. The combined treatment again exhibited superior efficacy, decreasing cell viability from 63.44% at 24 hours to 27.60% at 120 hours (Fig. 1e and 1f). Collectively, these data indicate that while both agents effectively suppress TNBC proliferation in a time-dependent manner, the honokiol + paclitaxel combination consistently outperforms each monotherapy across both cell lines.

Reversal of oncogenic miRNA-21 and restoration of tumor suppressors by honokiol and paclitaxel

The qRT-PCR analysis in MDA-MB-231 and MDA-MB-468 breast cancer cells revealed contrasting molecular effects for honokiol and paclitaxel. Honokiol significantly upregulated tumor suppressors PTEN and PDCD4 while suppressing oncogenic miRNA-21 (Fig. 2). Conversely, paclitaxel downregulated PTEN/PDCD4 and elevated miRNA-21. Notably, the honokiol + paclitaxel combination significantly reversed these paclitaxel-induced suppressions, significantly restoring PTEN (to 1.24 and 1.38 fold) and PDCD4 (to 0.86 and 1.36 fold), while mitigating miRNA-21 overexpression compared to paclitaxel monotherapy. Furthermore, all treatments significantly downregulated cyclin D1 and MMP-2 expression. Importantly, the combination exerted the strongest synergistic inhibition, driving cyclin D1 down to 61.6%

(MDA-MB-231) and 54.1% (MDA-MB-468), and MMP-2 down to 49.5% and 51.4% of controls, respectively, demonstrating its potent and robust anti-proliferative and anti-invasive efficacy.

Anti-proliferative effect of honokiol and paclitaxel combination associated with phospho-AKT reduction

Western blot analysis showed that total AKT protein expression remained constant across all groups in both cell lines. In MDA-MB-231 cells, honokiol, paclitaxel, and their combination clearly reduced phospho-AKT compared to controls ($p < 0.05$); however, the combination group showed no statistically significant difference compared to either honokiol or paclitaxel alone. In MDA-MB-468 cells, the combination group exhibited a significant reduction in phospho-AKT relative to honokiol alone, but not relative to paclitaxel alone (Fig. 3). Crucially, despite the lack of full statistical separation in the western blot, our previously performed MTT assays demonstrated that the combination group has a dramatically lower IC_{50} compared to each monotherapy. This strongly confirms that the combination exerts a more powerful synergistic effect on cell viability, and correlates with the pronounced downregulation of phospho-AKT, indicating an enhanced overall inhibition of the AKT pathway.

Enhanced anti-migratory effects of combined honokiol and paclitaxel in breast cancer

The anti-migratory effects of honokiol and paclitaxel, alone and in combination, were evaluated on MDA-MB-231 and MDA-MB-468 cell lines using a 24-hour wound healing assay. In both cell lines, the control and solvent groups maintained full migratory capacity (100% migration rate). Monotherapy with honokiol or paclitaxel significantly inhibited cell migration compared to the controls ($p < 0.05$), with MDA-MB-468 cells demonstrating greater sensitivity (honokiol: 46.73%; paclitaxel: 39.67%) than MDA-MB-231 cells (honokiol: 61.12%; paclitaxel: 53.88%). Notably, the combined treatment significantly enhanced this inhibitory effect, yielding the lowest migration rates of 44.52% and 32.50% for MDA-MB-231 and MDA-MB-468, respectively (Fig. 4a and 4b). These results indicate that the combination of honokiol and paclitaxel synergistically suppresses breast cancer cell migration.

Combination therapy with honokiol and paclitaxel reduces long-term colony formation

The clonogenic capacity of both MDA-MB-231 and MDA-MB-468 cells was significantly reduced by all treatments relative to the blank controls ($p < 0.05$). For MDA-MB-231 cells, monotherapies with honokiol and paclitaxel yielded relative colony counts of 37% and 34%, respectively. Similarly, in MDA-MB-468 cells, honokiol and paclitaxel reduced colony formation to 44% and 39% of the control (Fig. 4c and 4d). In both cell lines, the double combination (honokiol + paclitaxel) achieved the lowest colony counts, reducing formation to 29% in MDA-MB-231 and 31% in MDA-MB-468. This suggests that combining

honokiol and paclitaxel provides added benefit over monotherapy in inhibiting long-term colony formation in these breast cancer cell lines.

Increased apoptotic cell death by honokiol and paclitaxel combination therapy

The induction of apoptosis by honokiol, paclitaxel, and their combination was assessed in MDA-MB-231 and MDA-MB-468 breast cancer cells via Hoechst 33342 staining, a cell death ELISA, and a caspase-3 activity assay (Figs. 4 and 5). Hoechst staining revealed that, compared to the uniform intact nuclei in control and solvent groups, single-agent treatments induced characteristic apoptotic morphology, including chromatin condensation, pyknosis, and nuclear fragmentation. Notably, the honokiol and paclitaxel combination displayed the most severe nuclear disintegration. Quantitative ELISA analysis showed that honokiol and paclitaxel alone significantly increased apoptosis to 1.42 and 1.51 fold in MDA-MB-231, and to 1.66 and 1.72 fold in MDA-MB-468 cells, respectively ($p < 0.05$ vs. control). The combined treatment further enhanced apoptosis to 1.75 and 1.96 fold in the respective cell lines. Similarly, the caspase-3 activity assay demonstrated that honokiol and paclitaxel elevated enzyme activity to 1.83 and 1.71 fold in MDA-MB-231, and to 2.14 and 2.27 fold in MDA-MB-468 cells ($p < 0.05$). However, the honokiol and paclitaxel combination yielded the greatest activation of caspase-3, reaching 2.46 and 2.62 fold in MDA-MB-231 and MDA-MB-468 cells, respectively, which was significantly higher than controls and single-agent treatments ($p < 0.05$). Collectively, these results demonstrate that the honokiol and paclitaxel combination synergistically augments apoptotic cell death through enhanced DNA fragmentation and robust caspase-3 activation, exhibiting greater efficacy than monotherapies.

Discussion

The present study investigated the synergistic effects of honokiol and paclitaxel on MDA-MB-231 and MDA-MB-468 triple-negative breast cancer cells, focusing on miRNA-21/PTEN/PI3K/AKT signaling. Our findings demonstrate that honokiol enhances paclitaxel chemosensitivity through miRNA-21 downregulation, PTEN/PDCD4 restoration, and suppression of phospho-AKT, offering a novel strategy to overcome paclitaxel resistance.

Our MTT results revealed that honokiol and paclitaxel alone reduced cell viability dose-dependently in both cell lines, with MDA-MB-468 showing greater sensitivity than MDA-MB-231, consistent with established differences in drug responsiveness among triple-negative breast cancer subtypes [3]. The combination significantly lowered IC_{50} values from 6.22 to 4.21 μM (MDA-MB-231) and 5.03 to 3.21 μM (MDA-MB-468), indicating chemosensitization. This aligns with recent findings that honokiol potentiates conventional chemotherapeutics via multiple molecular targets [14, 18]. Combination index analysis confirmed synergism (CI < 1) across all fractional affected levels, with the strongest synergy at higher Fa values, supporting the Chou-Talalay model and suggesting that honokiol and paclitaxel act cooperatively rather than additively [19]. Our findings corroborate those of Han et al. [18], who demonstrated honokiol-induced synergy with paclitaxel in breast cancer through modulation of the miRNA-148a-5p-CYP1B1

axis. The time-course proliferation assays demonstrated that honokiol and paclitaxel monotherapies progressively inhibited cell growth over 120 hours, but the combination consistently outperformed either agent alone, reducing viability to 25.49% (MDA-MB-231) and 27.60% (MDA-MB-468). These results are in agreement with Yi et al. [19], who reported that honokiol enhances doxorubicin sensitivity in breast cancer via the miRNA-188-5p/FBXW7/c-Myc pathway, indicating that honokiol's chemosensitizing effects are not limited to paclitaxel but extend to multiple chemotherapeutic agents.

Gene expression analysis revealed a critical molecular dichotomy: honokiol downregulated miRNA-21 and upregulated PTEN and PDCD4, whereas paclitaxel alone exerted opposite effects, increasing miRNA-21 and suppressing PTEN/PDCD4. This paclitaxel-induced oncogenic miRNA upregulation is consistent with reports that chemotherapy can paradoxically activate survival pathways, including miRNA-21, contributing to drug resistance [6, 10]. Importantly, the combination reversed paclitaxel-induced miRNA-21 elevation, restoring PTEN and PDCD4 expression to levels comparable to or exceeding honokiol monotherapy. This suggests that honokiol counteracts the pro-survival effects of paclitaxel, thereby sensitizing cells to its cytotoxic action. Our results are supported by studies showing that miRNA-21 inhibition enhances paclitaxel efficacy in breast cancer cells [13], and that honokiol suppresses miRNA-21 in osteosarcoma via the PTEN/PI3K/AKT axis [12].

Both agents downregulated cyclin D1 and MMP-2, with the combination achieving the strongest inhibition (cyclin D1 to 61.6% and 54.1%; MMP-2 to 49.5% and 51.4% in MDA-MB-231 and MDA-MB-468, respectively). These findings corroborate the anti-proliferative and anti-invasive effects previously attributed to honokiol [14] and paclitaxel [4]. The pronounced suppression of cyclin D1, a key regulator of G1/S transition, and MMP-2, a critical enzyme for extracellular matrix degradation, provides a mechanistic basis for the observed inhibition of colony formation and migration. Our wound healing and colony formation assays confirmed that the combination significantly reduced migration rates to 44.52% (MDA-MB-231) and 32.50% (MDA-MB-468) and colony formation to 29% and 31%, respectively, surpassing monotherapies. These findings align with studies demonstrating honokiol's ability to inhibit breast cancer metastasis through EMT blockade [14].

Apoptosis evaluation via Hoechst staining, ELISA, and caspase-3 activity showed that the combination induced the most pronounced apoptotic morphology, highest nucleosome enrichment (1.75 and 1.96 fold), and greatest caspase-3 activation (2.46 and 2.62 fold) in both cell lines. These results are consistent with honokiol's established pro-apoptotic mechanisms, including modulation of Bcl-2 family proteins and caspase cascade activation [16]. The enhanced apoptosis observed with the combination may be attributed to honokiol-mediated suppression of survival signals (PI3K/AKT) and restoration of tumor suppressors (PTEN, PDCD4), thereby creating a permissive environment for paclitaxel-induced cytotoxicity. Importantly, despite the combination group not showing statistically significant differences in p-AKT reduction compared to paclitaxel alone in MDA-MB-468 cells, the MTT results demonstrated a dramatically lower IC_{50} for the combination, indicating that the observed synergistic cytotoxic effect is not solely dependent on AKT phosphorylation status but may involve additional downstream targets or

parallel pathways. This highlights the complexity of the molecular interactions and suggests that honokiol may act through multiple mechanisms to enhance paclitaxel efficacy.

The mechanistic basis for the observed synergy centers on the miRNA-21/PTEN/PI3K/AKT axis. MiRNA-21 is a well-known oncomiR that targets PTEN and PDCD4, leading to constitutive PI3K/AKT activation and chemoresistance [8, 10, 11]. Our qRT-PCR results demonstrate that honokiol downregulates miRNA-21, thereby relieving PTEN and PDCD4 from translational repression. This is consistent with findings in osteosarcoma where honokiol suppressed miRNA-21 and activated the PTEN/PI3K/AKT pathway [12]. The restoration of PTEN, a lipid phosphatase that dephosphorylates PIP3, inhibits AKT activation by preventing its recruitment to the plasma membrane [12]. The subsequent reduction in phospho-AKT, as observed in our Western blots, correlates with decreased downstream survival signaling. It is important to note that in our Western blot analysis, total AKT levels remained constant across all groups, validating the use of total AKT as a proper loading control, as recommended in the literature for phospho-AKT measurements [25]. This ensures that the observed p-AKT changes reflect true phosphorylation status rather than variations in protein expression.

Paclitaxel alone elevated miRNA-21 and suppressed PTEN/PDCD4, a paradoxical effect previously documented as an adaptive survival response to microtubule-targeting agents [6, 13]. This paclitaxel-induced miRNA-21 upregulation may contribute to the development of acquired resistance. Honokiol reverses this effect, thereby abrogating the pro-survival feedback loop. The combination's ability to maintain PTEN and PDCD4 levels while simultaneously reducing cyclin D1 and MMP-2 expression further reinforces the anti-proliferative and anti-invasive phenotype. Cyclin D1 is a downstream target of PI3K/AKT signaling, and its downregulation impedes G1/S progression, aligning with the observed growth inhibition. MMP-2, also regulated by AKT and NF-κB, is essential for tumor invasion; its suppression explains the reduced migratory capacity. Additionally, honokiol has been shown to inhibit NF-κB activation [17], which could further contribute to the downregulation of MMP-2 and cyclin D1, as both genes are transcriptionally regulated by NF-κB. This dual targeting of PI3K/AKT and NF-κB pathways by honokiol likely amplifies paclitaxel's cytotoxic effects. Moreover, honokiol induces apoptosis through Bcl-2 modulation and caspase activation [16], while paclitaxel promotes mitotic arrest and apoptosis; the combination triggers both intrinsic and extrinsic apoptotic pathways, as evidenced by increased caspase-3 activity and DNA fragmentation. Thus, the synergistic interaction is mechanistically grounded in the coordinated modulation of miRNA-21/PTEN/PI3K/AKT, NF-κB, and apoptotic pathways.

This study is limited to in vitro models using two TNBC cell lines; in vivo validation is lacking. The 24-hour treatment window may not capture long-term effects. Normal cell toxicity was not assessed, and the molecular mechanisms were not confirmed by knockout or inhibitor studies. Additionally, the exact binding interaction between honokiol and miRNA-21 remains undefined.

Conclusion

Honokiol synergistically enhances paclitaxel cytotoxicity in triple-negative breast cancer by downregulating miRNA-21, restoring PTEN and PDCD4, and suppressing phospho-AKT and downstream oncogenic targets (cyclin D1, MMP-2). This combination also inhibits migration, colony formation, and induces apoptosis, offering a promising strategy to overcome paclitaxel resistance. Future studies should validate these findings in vivo using orthotopic breast cancer models and assess honokiol's bioavailability, toxicity, and optimal dosing. Molecular docking and miRNA target validation experiments are needed to elucidate direct interactions. Clinical trials exploring honokiol-paclitaxel combination therapy in TNBC patients are warranted.

Abbreviations

ABTS
2,2'-azino-bis(3-ethylbenzothiazoline-6-sulfonic acid)
Akt
Protein kinase B
ANOVA
Analysis of variance
Bak
Bcl-2 antagonist/killer 1
Bax
Bcl-2-associated X protein
Bcl-2
B-cell lymphoma 2
Bcl-w
B-cell lymphoma-w
Bcl-xL
B-cell lymphoma-extra large
BH3
Bcl-2 homology 3
BRCA
Breast cancer susceptibility gene
cDNA
Complementary DNA
CI
Combination index
CO_2
Carbon dioxide
C-PC
C-Phycocyanin
DEVD-pNA

N-acetyl-Asp-Glu-Val-Asp-p nitroanilide

DMSO

Dimethyl sulfoxide

DNA

Deoxyribonucleic acid

DTT

Dithiothreitol

ECL

Enhanced chemiluminescence

EDTA

Ethylenediaminetetraacetic acid

EGFR

Epidermal growth factor receptor

ELISA

Enzyme-linked immunosorbent assay

ER

Estrogen receptor

Fa

Fraction affected

FBS

Fetal bovine serum

GSK3β

Glycogen synthase kinase-3 beta

HER2

Human epidermal growth factor receptor 2

HRP

Horseradish peroxidase

IC_{50}

Half maximal inhibitory concentration

JNK

c-Jun N-terminal kinase

MAPK

Mitogen-activated protein kinase

Mcl-1

Myeloid cell leukemia-1

MMLV

Moloney murine leukemia virus

MMP-2

Matrix metalloproteinase-2

MMP-9

Matrix metalloproteinase-9

mTOR

Mammalian target of rapamycin

MTT

3-(4,5-dimethylthiazol-2-yl)-2,5-diphenyltetrazolium bromide

NaCl

Sodium chloride

P53

Tumor protein p53

PARP

Poly (ADP-ribose) polymerase

PBS

Phosphate-buffered saline

PD-L1

Programmed death-ligand 1

PI3K

Phosphatidylinositol 3-kinase

PR

Progesterone receptor

PTEN

Phosphatase and tensin homolog

PVDF

Polyvinylidene difluoride

qRT-PCR

Quantitative real-time polymerase chain reaction

RB1

Retinoblastoma 1

RNA

Ribonucleic acid

ROS

Reactive oxygen species

RPMI

Roswell Park Memorial Institute

SD

Standard deviation

SDS

Sodium dodecyl sulfate

SDS-PAGE

Sodium dodecyl sulfate–polyacrylamide gel electrophoresis

TNBC

Triple-negative breast cancer
Tris-HCl
Tris(hydroxymethyl)aminomethane hydrochloride
Wnt
Wingless/Int-1.

Declarations

Ethical approval

This study did not involve human participants or animal experimentation. The research utilized the commercially available human MDA-MB-231 and MDA-MB-468 breast cancer cell lines. All experimental protocols were conducted in accordance with relevant institutional guidelines and regulations. The study design and ethical considerations were reviewed and approved by the Ethics Committee of AUMS (Approval Code: IR.ARAKMU.REC.1398.194).

Conflict of interest

The authors declare that they have no conflicts of interest to disclose.

Funding

This work was supported by a grant from the Traditional and Complementary Medicine Research Center from Arak University of Medical Sciences (AUMS) of Iran [Grant number 3473].

Author Contribution

ZS, SMJH and HK; Conceptualization, Investigation, Methodology, Formal analysis and writing original draft preparation. HK and SMJH; Resources, Supervision, Editing, and funding acquisition. All authors read and approved the final manuscript.

Acknowledgement

The authors thank the Molecular and Medicine Research Center, AUMS, for providing the necessary equipment for this work.

Data availability statement

The data underlying this article are available in the article and in its online supplementary material.

References

1. Sung H et al (2021) Global Cancer Statistics 2020: GLOBOCAN Estimates of Incidence and Mortality Worldwide for 36 Cancers in 185 Countries. CA Cancer J Clin 71(3):209–249
2. Bray F et al (2024) Global cancer statistics 2022: GLOBOCAN estimates of incidence and mortality worldwide for 36 cancers in 185 countries. CA Cancer J Clin 74(3):229–263
3. Medina MA et al (2020) Triple-Negative Breast Cancer: A Review of Conventional and Advanced Therapeutic Strategies. Int J Environ Res Public Health, 17(6)
4. Orr GA et al (2003) Mechanisms of Taxol resistance related to microtubules. Oncogene 22(47):7280–7295
5. Nedeljković M, Damjanović A (2019) Mechanisms of Chemotherapy Resistance in Triple-Negative Breast Cancer-How We Can Rise to the Challenge. Cells, 8(9)
6. Najjary S et al (2020) Role of miR-21 as an authentic oncogene in mediating drug resistance in breast cancer. Gene 738:144453
7. Dziechciowska I et al (2023) miRNA Expression Profiling in Human Breast Cancer Diagnostics and Therapy. Curr Issues Mol Biol 45(12):9500–9525
8. Si ML et al (2007) miR-21-mediated tumor growth. Oncogene 26(19):2799–2803
9. Liu X et al (2022) Potential utility of miRNAs for liquid biopsy in breast cancer. Front Oncol 12:940314
10. Akhtarkhavari T, Bahrami AR, Matin MM (2022) Downregulation of miR-21 as a promising strategy to overcome drug resistance in cancer. Eur J Pharmacol 932:175233
11. Kuang Y, Nie YJ (2016) Exploration of the regulatory effect of miR-21 on breast cancer cell line proliferation and invasion as well as the downstream target genes. Asian Pac J Trop Med 9(5):470–473
12. Yang J, Zou Y, Jiang D (2018) Honokiol suppresses proliferation and induces apoptosis via regulation of the miR–21/PTEN/PI3K/AKT signaling pathway in human osteosarcoma cells. Int J Mol Med 41(4):1845–1854
13. Mei M et al (2010) Downregulation of miR-21 enhances chemotherapeutic effect of taxol in breast carcinoma cells. Technol Cancer Res Treat 9(1):77–86
14. Mottaghi S, Abbaszadeh H (2022) Natural Lignans Honokiol and Magnolol as Potential Anticarcinogenic and Anticancer Agents. A Comprehensive Mechanistic Review. Nutr Cancer 74(3):761–778
15. Singh SK et al (2026) Honokiol and Its Emerging Role in Breast Cancer Therapy. Cancers (Basel), 18(12)
16. Battle TE, Arbiser J, Frank DA (2005) The natural product honokiol induces caspase-dependent apoptosis in B-cell chronic lymphocytic leukemia (B-CLL) cells. Blood 106(2):690–697

17. Ahn KS et al (2006) Honokiol potentiates apoptosis, suppresses osteoclastogenesis, and inhibits invasion through modulation of nuclear factor-kappaB activation pathway. Mol Cancer Res 4(9):621–633
18. Han X et al (2024) Honokiol Exhibits Anti-Tumor Effects in Breast Cancer by Modulating the miR-148a-5p-CYP1B1 Axis. Am J Chin Med 52(6):1843–1861
19. Yi X et al (2021) *Honokiol antagonizes doxorubicin resistance in human breast cancer via miR-188-5p*/FBXW7/c-Myc pathway. Cancer Chemother Pharmacol, 87(5): pp. 647–656
20. Zhang B et al (2020) Targeting miRNAs by natural products: A new way for cancer therapy. Biomed Pharmacother 130:110546
21. Nazmabadi R et al (2024) Dihydroartemisinin Enhances the Therapeutic Efficacy of BH3 Mimetic Inhibitor in Acute Lymphoblastic Leukemia Cells via Inhibition of Mcl-1. Asian Pac J Cancer Prev 25(1):325–332
22. Abbasi Y et al (2024) Formononetin and Dihydroartemisinin Act Synergistically to Induce Apoptosis in Human Acute Myeloid Leukemia Cell Lines. Cell J 26(2):121–129
23. Amini R, Karami H, Bayat M (2021) Combination Therapy with PIK3R3-siRNA and EGFR-TKI Erlotinib Synergistically Suppresses Glioblastoma Cell Growth In Vitro. Asian Pac J Cancer Prev 22(12):3993–4000
24. Ashofteh N et al (2021) MiRNA-Mediated Knock-Down of Bcl-2 and Mcl-1 Increases Fludarabine-Sensitivity in CLL-CII Cells. Asian Pac J Cancer Prev 22(7):2191–2198
25. Sarbassov DD et al (2005) Phosphorylation and regulation of Akt/PKB by the rictor-mTOR complex. Science 307(5712):1098–1101

Figures

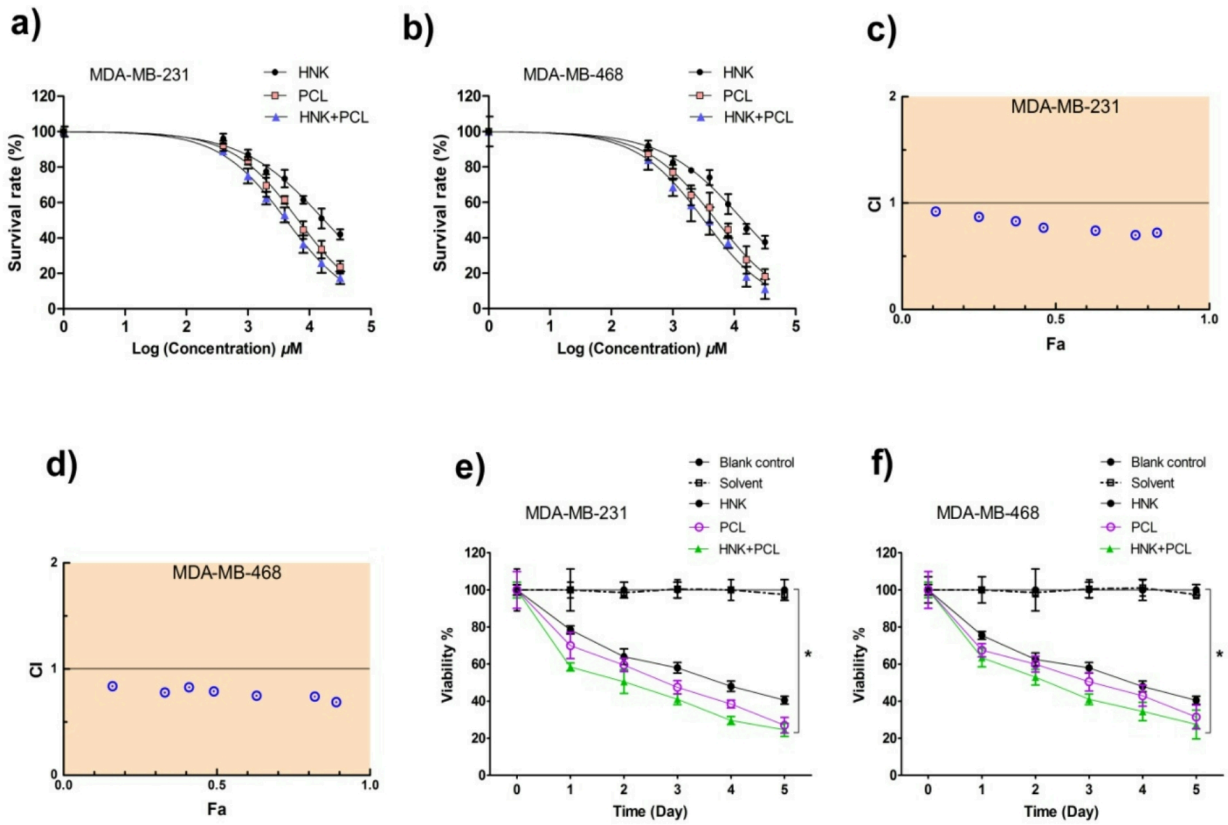


Figure 1

Synergistic cytotoxic and anti-proliferative effects of Honokiol (HNK) and Paclitaxel (PCL) in MDA-MB-231 and MDA-MB-468 triple-negative breast cancer cells.

(a, b) Dose-response cell survival curves determined by MTT assay after 24 h of treatment with HNK, PCL, or their combination (HNK+PCL) in MDA-MB-231 (a) and MDA-MB-468 (b) cells. **(c, d)** Combination index (CI) analysis using the Chou-Talalay method for MDA-MB-231 (c) and MDA-MB-468 (d) cells. CI values < 1 indicate synergistic interactions across various fractional affected (Fa) levels. **(e, f)** Time-dependent anti-proliferative effects assessed by trypan blue exclusion assay. Cell viability was measured over 120 hours (5 days) in MDA-MB-231 (e) and MDA-MB-468 (f) cells. Data are presented as mean ± SD from at least three independent experiments. $^{*}p<0.05$ vs. control or single-agent treatment groups.

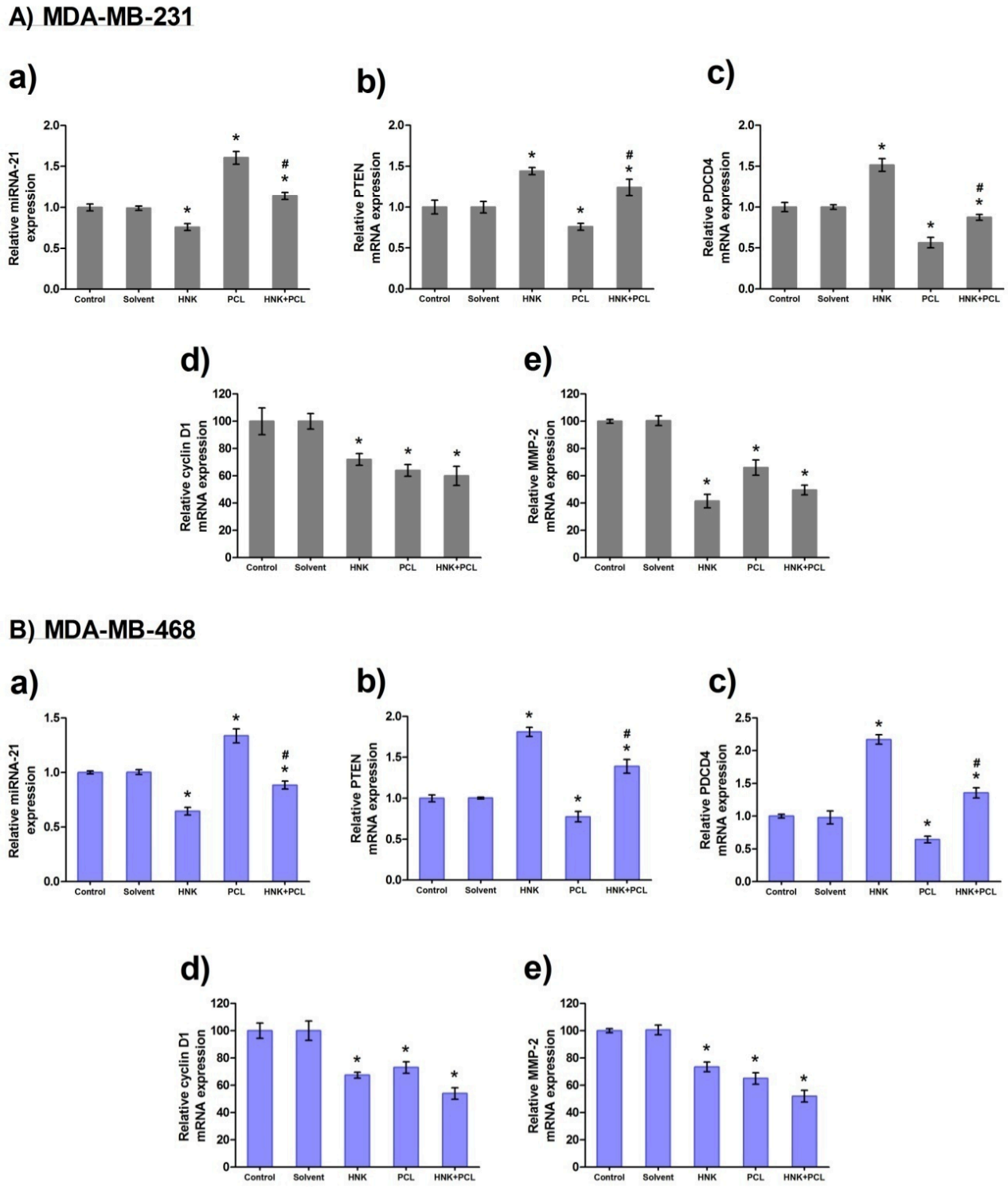


Figure 2

Modulation of the miRNA-21/PTEN/PDCD4 axis and downstream target genes by Honokiol (HNK) and Paclitaxel (PCL) in MDA-MB-231 and MDA-MB-468 breast cancer cells. (A, B) Quantitative real-time PCR (qRT-PCR) analysis of mRNA expression levels of oncogenic miRNA-21 (a), tumor suppressors PTEN (b) and PDCD4 (c), and proliferation/invasion-related genes Cyclin D1 (d) and MMP-2 (e) in MDA-MB-231 (A) and MDA-MB-468 (B) cells. Cells were treated with IC_{50} concentrations of HNK, PCL, or their

combination (HNK+PCL) for 24 h. β-actin was used as the internal reference gene, and relative expression was normalized to the untreated control group (set to 1.0).
Data are presented as mean ± SD from at least three independent experiments. *p<0.05 vs. control group; #p<0.05 vs. PCL-treated group

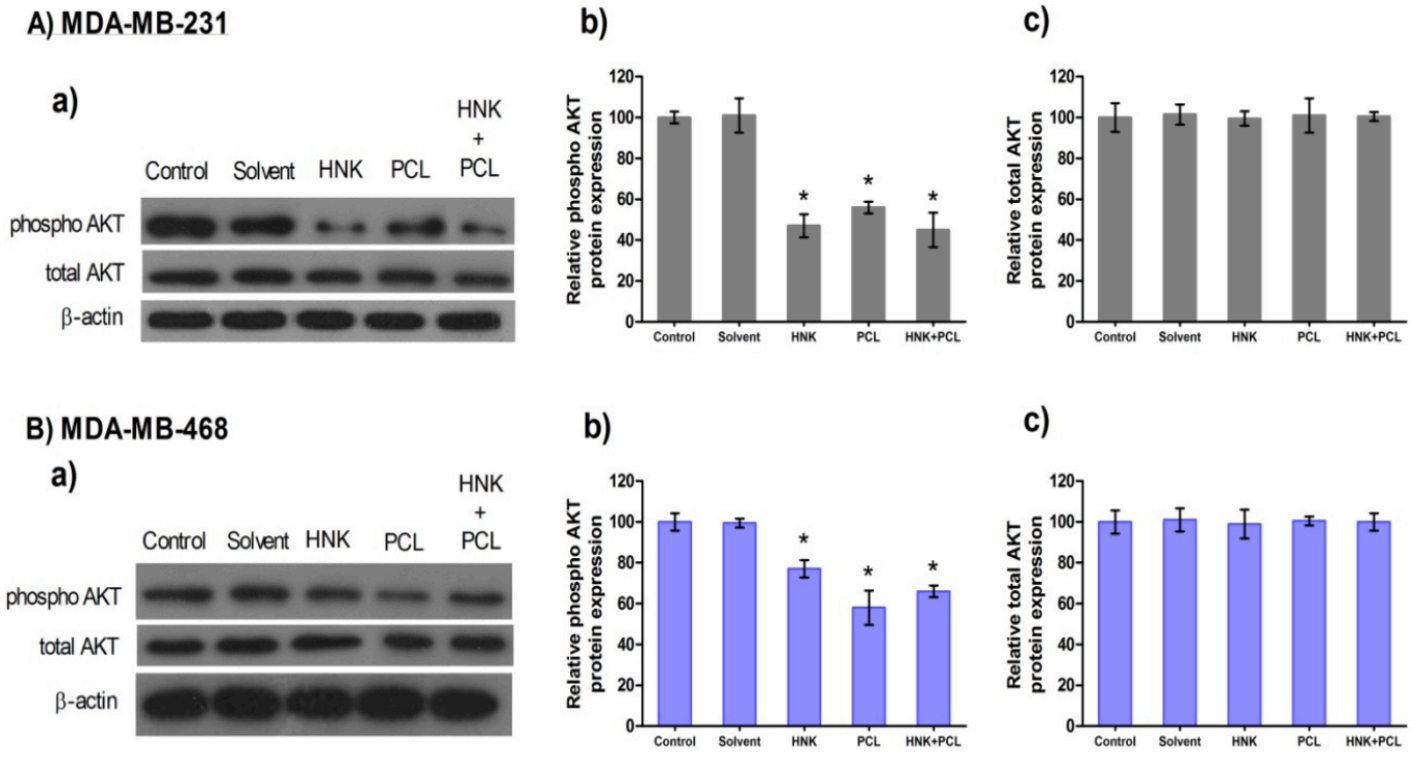


Figure 3

Honokiol (HNK) and Paclitaxel (PCL) combination inhibits the PI3K/AKT signaling pathway in MDA-MB-231 and MDA-MB-468 breast cancer cells.
(A, B) Western blot analysis of phospho-AKT and total AKT protein expression in MDA-MB-231 (A) and MDA-MB-468 (B) cells after 24 h treatment with IC_{50} concentrations of HNK, PCL, or their combination (HNK+PCL). β-actin was used as an internal loading control. Representative Western blot images are shown in **(a)**, and densitometric quantification of relative phospho-AKT **(b)** and total AKT **(c)** protein expression normalized to β-actin are presented as bar graphs. Data are presented as mean ± SD from at least three independent experiments. Statistical significance was determined by one-way ANOVA followed by Tukey's post-hoc test. *p<0.05 vs. control group.

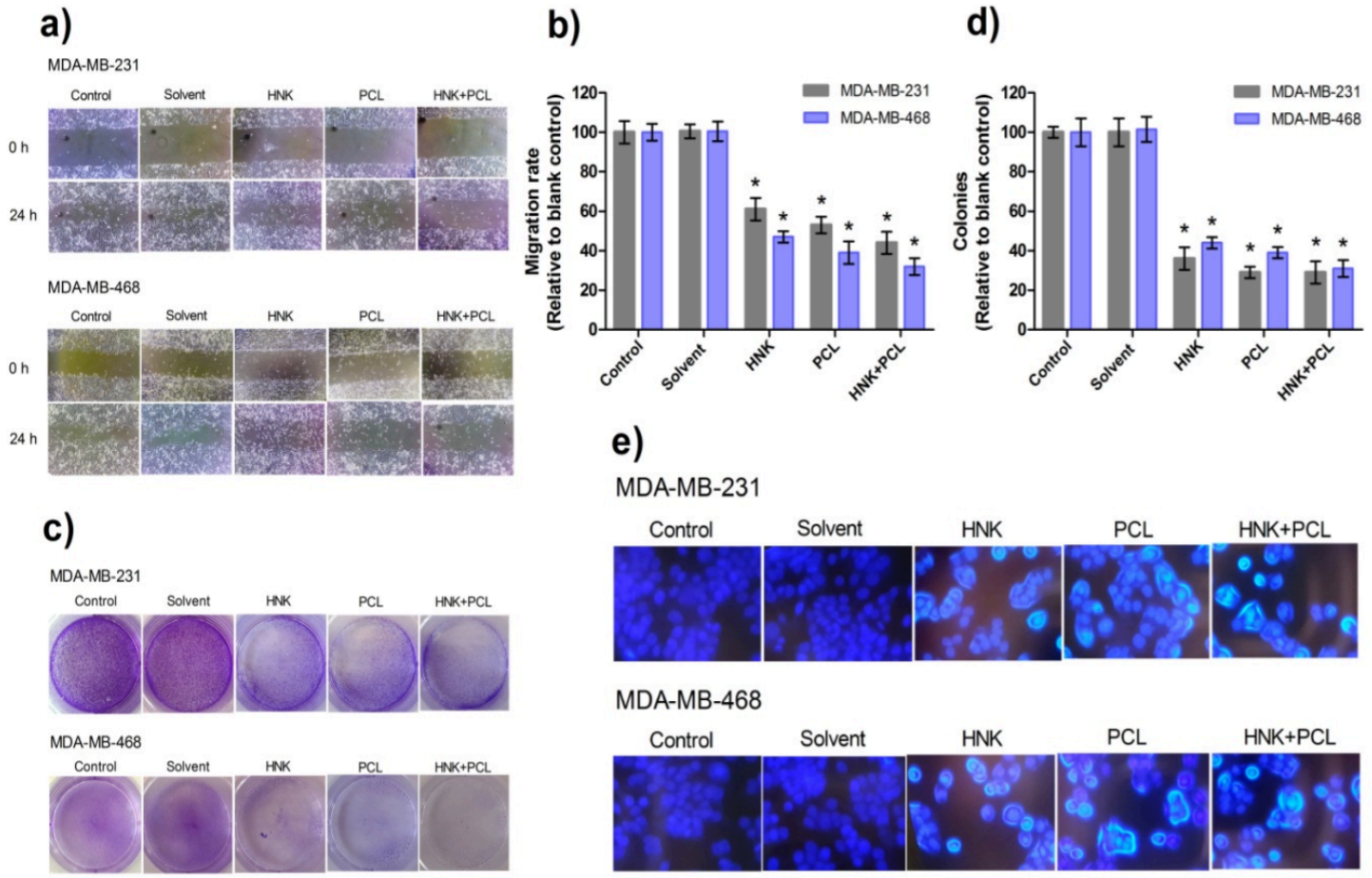


Figure 4

Honokiol (HNK) and Paclitaxel (PCL) combination suppresses migration and clonogenic survival, and induces apoptotic morphology in MDA-MB-231 and MDA-MB-468 breast cancer cells. **(a)** Representative images of the wound healing assay captured at 0 h and 24 h post-treatment in both cell lines.
(b) Quantification of the cell migration rate, expressed as a percentage relative to the blank control in both cell lines. **(c)** Representative images of the colony formation assay stained with crystal violet after 14 days of incubation.
(d) Quantification of colony numbers, expressed as a percentage relative to the blank control.
(e) Representative fluorescence microscopy images of Hoechst 33342-stained cells. Data are presented as mean ± SD from at least three independent experiments. $^{*}p<0.05$ vs. control group.

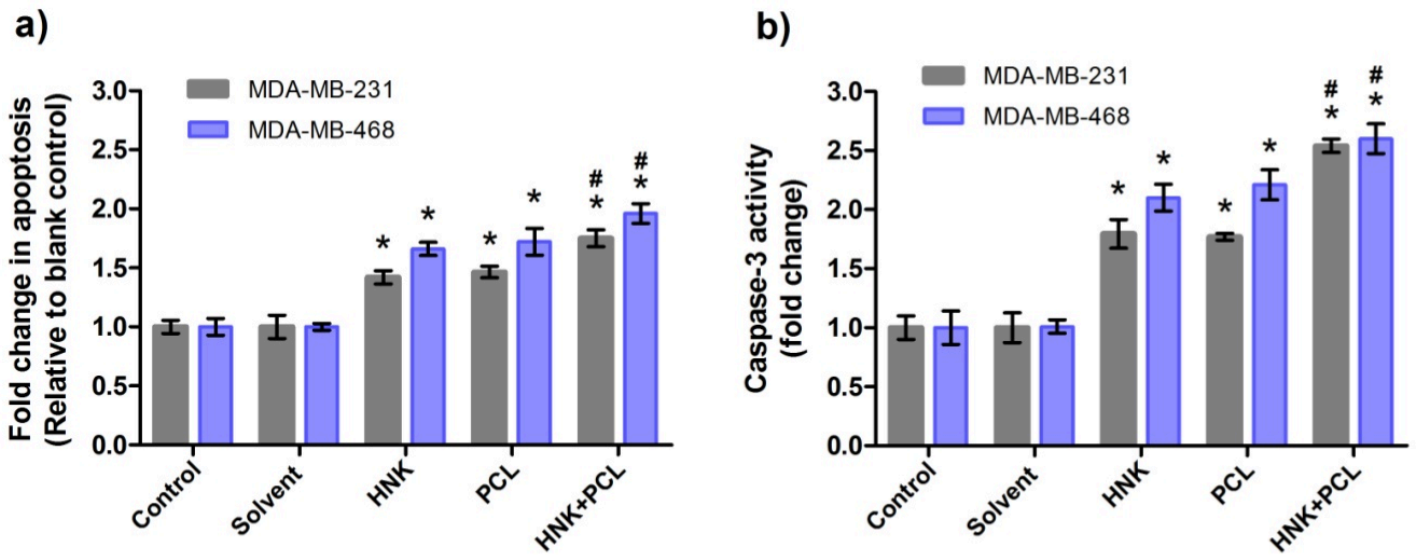


Figure 5

Honokiol (HNK) and Paclitaxel (PCL) combination synergistically enhances apoptotic cell death in MDA-MB-231 and MDA-MB-468 breast cancer cells. **(a)** Apoptosis was quantified using an ELISA-based cell death detection kit, measuring the fold change in cytoplasmic mono- and oligonucleosomes relative to the blank control after 24 h of treatment. **(b)** Caspase-3 activity was evaluated using a colorimetric assay (DEVD-pNA cleavage) and is presented as the fold change relative to the blank control. Cells were treated with IC_{50} concentrations of HNK, PCL, or their combination (HNK+PCL) for 24 h. Data are presented as mean ± SD from at least three independent experiments. $^{*}p<0.05$ vs. control group; $^{\#}p<0.05$ vs. single-agent treatment groups.